Experimental Study on Jets Formed Under Discharges of High-Pressure Subcooled Water and Steam-Water Mixture

F. Masuda, T. Nakatogawa
Plant Engineering Dept., Mitsubishi Atomic Power Industries, Inc., 4-1, Shibakoen 2-chome, Minato-ku, Tokyo, Japan

K. Kawanishi, M. Isono
Takasago Technical Institute, Mitsubishi Heavy Industries, Ltd., Takasago, Hyogo, Japan

Abstract

An experimental study on characteristics of jet formed under steady discharges of high-pressure subcooled water and two-phase mixture has been performed. The experiments were carried out with typical stagnation pressure 2.05 and 4.02 MPa and stagnation enthalpy ranging from about 500 to 2800 kJ/kg. Measurements were made of discharged flow rate, nozzle exit pressure, jet impingement force, and recovery pressure distribution on free and impingement jet. Two circular nozzles (5mm I.D.) with round and sharp edge entrance and an elliptical nozzle (10mm × 2.5mm) were used. Typical measured data are shown, and based on each measured parameter, dependences on upstream stagnant enthalpy, nozzle geometry and axial distance of jet are described. Principal results for each measured parameter are as follows.

(1) Discharged flow rate: Flow rate data show, in comparison with predictions by representative critical flow models, that Hanry-Fauske's model can be in better agreement, and an influence of nozzle entrance geometry is little distinctive except for the highly subcooled region.

(2) Impingement force: Thrust coefficients based on the data for the round edge entrance nozzle are about 1.1∿1.2 in the saturated region and approach about 1.95 in the subcooled region with decreasing the stagnation enthalpy. A reduction effect of sharp edge entrance is distinctive, about 20%, in the highly subcooled region and the saturated region.

(3) Recovery pressure distribution of jet: The data of axial and radial distributions show that characteristics of expansion and pressure decay highly depend on the stagnation enthalpy. For the subcooled water, a prominent core of high pressure, which is accompanied with oscillation and rapidly reduces with increasing the axial distance, is obseved. A marked expansion with very low pressure reults when it vanishes. A rate of pressure decay increases and an intensity of oscillation is mitigated with increasing stagnation enthalpy. For the two-phase region, on the other hand, expansion and pressure decay initiates just downstream of the nozzle exit and a dependence of the decay on the stagnation enthalpy is small.

1. Introduction

In the evaluation of effects caused by a postulated pipe rupture accident in a nuclear power plant, it is important to know the parameters such as discharged flow rate, fluid reaction, and jet impingement force and pressure distribution as they have serious effects on the structures, equipments and the other components in the design.

With respect to a blowdown of high energy fluid, recent theoretical and experimental investigations have detailedly clarified fluid behaviors within a flow passage, in particular noticing a nonequilibrium condition for subcooled water. On the other hand, as to characteristics of jet formed outside the flow passage, the work up to now has not been enough to establish applicable evaluation methods in the design basis. In view of this, experimental studies on jet have been performed. In previous studies, experiments on a transient subcooled water blowdown and a steady steam blowdown were carried out. [1][2]

In order to more clarify characteristics of jet in relation to upstream condition, at present, the experiments were carried out under steady discharges of subcooled water and steam-water mixture. Measurements were made of discharge flow rate, nozzle exit pressure, jet impingement force, and three dimensional pressure distributions on free and impingement jets.

Typical measured data are shown, and based on each measured parameter, influences of upstream stagnant conditions, nozzle geometry and axial distance of jet are described.

2. Experimental apparatus and procedure

Experiments were carried out in steady flow condition. A schematic diagram of the apparatus is shown in Fig. 1. Water is pressureized and transported by pumps and heated up through a heat exchanger, and then ejected through a nozzle into a test vessel in which the pressure is kept near the atmosphere. The amplitude of pressure pulsation caused by the pump is suppressed by an accumulator to be within one percent. In the case of discharge of steam-water mixture, the mixture is generated through a mixer by mixing water with steam from a high-pressure boiler. The typical test stagnation pressure are 2.05 and 4.02 MPa at the entrance of nozzle.

The discharged flow rate is measured with two orifice flow meters located in the outlet of the pump and in the steam line.

In the test of impingement jet, the jet is impinged vertically on a target plate which is set up horizontally and designed to be continuously movable horizontally along two axes and vertically to permit the measurement of three-dimensional pressure distributions. The impingement force is measured with three load cells attached to the target plate. The pressure distribution on the target plate is measured with a pressure tap located at the center of it. In the test of free jet, the pressure distribution is measured with the Pitot tube fixed on the target plate.

Three nozzles shown in Fig. 2(a-c) were used: two cirular nozzles are inner diameter 5mm, and one has round entrance and the other sharp edge entrance. An elliptical nozzle, which is used for only the test of jet, is major diameter 10mm and minor diameter 2.5mm. Each of nozzles has a constant area section 10mm long of which roughness is about 1μm.

3. Experimental Results and Discussion

3.1 Discharged Flow Rate and Nozzle Exit Pressure

Measured discharge flow rate data are plotted in Fig. 3 with stagnation pressure 2.05 and 4.02 MPa for the round edge entrance nozzle, and 2.05 MPa for the sharp edge entrance nozzle. Discharge flow in the present experiment can be regarded as a critical flow condition. Many investigations of critical flow have been performed theoretically and experimentally. Here, predictions by three representative theoretical models for an ideal nozzle are compared with the data for the round entrance nozzle: homogeneous equilibrium model, Moody's model [3](for only saturated region) and Henry-Fauske's model [4]. As shown in Fig. 3, Henry-Fauske's model is in good agreement throughout the whole region, homogeneous equilibrium model tends to underestimate, and Moody model tends to overestimate in the low quality region. Comparing the data for the sharp edge entrance nozzle with that for the round entrance nozzle, appreciable difference is not seen except highly subcooled region.

Measured pressures at the nozzel exit of the round and sharp edge entrance nozzle are plotted in Fig. 4 for the stagnation pressure 2.05 MPa. The difference between the round and sharp edge nozzle is distinctive in the subcooled region: the exit pressure of the sharp entrance nozzle are much lower than of the round entrance nozzle. This indication in the sharp entrance nozzle would be attributed to the occurrence of metastable core separated from the nozzle wall, since the measured pressure is at the wall surface. In addition, the predicted exit pressure, namely, critical pressure by Henry-Fauske's model is shown in Fig. 4. Comparing the data of the round entrance nozzle, the date near the point of saturated water are lower than the prediction.

3.2 Jet Impingement Force

Impingement force, namely, the reaction force of the target plate under the steady discharge is expressed theoretically as following.

$$F = \left(\frac{V_e G^2}{g} + P_e - P_\infty\right) A_e \qquad (1)$$

where F: impingement force, V_e: exit specific volume,
G: mass flow rate, g: gravitational constant, P_e: exit pressure,
P_∞: ambient pressure ($\sim$101.3 kPa), Ae: discharge area.
Another simplified formula in term of thrust coefficient is often used in the design evaluation:

$$F = (C_T P_o - P_\infty) A_e$$

where C_T: thrust coefficient, P_o: stagnation pressure upstream of nozzle. The thrust coefficients calculated by substituting the measured data for the stagnation pressure 2.05 MPa to eq. (2) are plotted in Fig. 5. For the round entrance nozzle, the thrust coefficients approach about 1.95 in the highly subcooled region and decrease with incresing the stagnation enthalpy, and then in the two-phase region calm down to about 1.1∿1.2. For the sharp entrance nozzel, on the other hand, the thrust coefficients approach about 1.5 in the subcooled region and calm down to about 0.9 in the two-phase region, and comparing with that of the round entrance nozzle, about 20% reduction exists in the highly subcooled region and the two-phase region. Furthermore, variation of theoretical thrust coefficient is shown in Fig. 5 applying critical flow parameters of Henry-Fauske's model to eq.(1) and coupling with eq. (2). Comparing with plotted data of round entrance nozzle, it is in good agreement.

3.3 Recovery Pressure Profile of Jet

3.3.1 Jet from the Circular Nozzle

Radial pressure profiles at the typical distances are shown in Fig. 6 (a-c) for subcooled water and two-phase with stagnation pressure 4.02 MPa. For the case of subcooled water shown in Fig. 6(a), abrupt expansion does not occure just downstream of the nozzle exit; but once oscillation occurs , steep reduction of prominent central portion progresses with increase of axial distance, and then expansion in a periphery with very low pressure is observed. When the central peak vanishes, a marked expansion results with very low pressure and almost flat distribution, and in farther distance gradual expansion continues with increase of distance. For the case of two-phase of very low quality shown in Fig.(c), on the other hand, it is observed that an abrupt expansion occurs just downstream of the nozzle exit, and a decay of central peak is faster than for the case of subcooled water, and intensity of oscillation is more mitigated. Comparing Fig. 6(a) with Fig. 6(b), though the stagnation enthalpy is slightly different (∿3%), the impingement jet has the longer high pressure region on the axis than that of free jet.

Variation of central pressure along the jet axis are shown in Fig. 7 on free jets, and in Fig. 8 on impingement jets for various stagnation enthalpies with stagnation pressure 4.02 MPa. These figures more clearly show the dependence of pressure decay on stagnation enthalpy. Difference of pressure decay between the two-phase of very low quality and the saturated steam is small on both the free and impingement jets, and an effect of impingement is also small.

Here, noticing the profile variation in the case of subcooled water, the prominent central portion can be regarded as a "flashing core", since the jet is superheated by abrupt depressurization to the ambient pressure and then is accompanied with a bubble occurence and growth which trigger a breakup of jet. It may be, though, bold to image a structure of jet by only the pressure

profile, a stable profile just downstream of the nozzle exit would indicate being in the stage of bubble occurence, and an oscillatory profile would indicate being in a transition from an abrupt bubble growth to the breakup of liquid phase which causes droplets, and a vanishment of central peak would show that an equilibrium mist flow is substantially accomplished. Lienhard and Day [5] studied the breakup of superheated liquid jet from the small orifices (1/32∿1/8-in-dia) and obtained correlations of breakup length noticing the bubble growth and approximating 'a jet shatters when a bubble radius grows up to about nozzle diameter'; however, it would be inappropriate to extend this assumption to a large scale nozzle. For the large nozzle, the bubble radius which triggers the breakup might be remarkably small comparing with nozzle diameter, and this might lead to that a scale effect becomes negligible.

We found an approximation of central pressure decay on the jet axis in the steep decay region:

$$\frac{P_c - P_\infty}{P_o - P_\infty} = \exp\left[-A\left(\frac{H - L_b - Limp}{D}\right)^2\right] \qquad (3)$$

(if greater than 1.0 → 1.0)

where P_c: central recovery pressure of jet, A: constant depending on the superheat, H: distance from the nozzle exit, L_b: breakup length where the droplets occur at the center of jet, Limp: delayed length caused by impingement (taken for only subcooled water and impingement jet). For constant 'A', assuming that a process of steep dacay would be mainly governed by thermal diffusion from liquid to bubbles and then from droplets to vapor, and based on the data,

$$A \simeq \left(\frac{Ja}{1290}\right)^2 \qquad (4)$$

where Ja is Jakob number. Furthermore, considering that Ja is nearly proportional to superheat, and adding a term for two-phase region based on the data,

$$A \simeq \frac{(To - T_\infty)^2}{1.29 \times 10^5} + 0.33 x_o^{0.15} \qquad (5)$$

where To: temperature upstream of nozzle(°C), T_∞: saturation temperature at ambient pressure (°C), x_o: stagnant quality upstream of nozzle.
Considering the bubble growth by heat conduction, L_b is approximated as [6]

$$L_b \simeq U_e \cdot \left(\frac{R_b}{Ja}\right)^2 \cdot \pi \alpha_\ell \qquad (6)$$

where U_e: velocity at the nozzle exit, R_b: bubble radius causative of breakup (unknown well), α_ℓ: thermal diffusivity of liquid. Caluculated results using eq.(3) and (5) for free jets are shown in Fig. 7 assuming 2mm as R_b which is equivalent to average of used nozzle diameters in Lienhard and Day's study.
On the other hand for impingement jet, at present, it is difficult to obtain correlations of 'Limp' to upstream condition and nozzle diameter. Conversely, Limp's obtained from best-fitting, which is shown in Fig. 8, with data for

h_o = 720, 904, 1076 kJ/kg are 3.2 2.7, 2.4 as Limp/D. They are in tendency of decreasing with increase of stagnation enthalpy.

3.3.2 Jet from the Elliptical Nozzle

For impingement jet, pressure profiles along the major and minor axis are shown in Fig. 9 for subcooled water with stagnation pressure 4.02 MPa, and variations of central pressure along the jet axis in Fig. 10 for various stagnation enthalpies.

In Fig. 9, the flashing core and its reduction with increasing of axial distance are observed as well as the case of circular nozzle, and then a difference of core profile between major and monor axis becomes small with reduction. For the case of two-phase (h_o = 1378 kJ/kg), non-axsymmetric profiles of which the expansion on the minor axis is greater than on the major axis are observed in farther downstream of nozzle after becoming axsymmetric near the nozzle exit (H $\sim$10 mm).

In Fig. 10, pressure decay becomes faster and pressure oscillation is more mitigated with increasing the stagnation enthalpy. This tendency is similar to the case of circular nozzle and the decay slope for the two-phase region is very close to that of the circular nozzle; however, for the case of subcooled water, delay of decay near the nozzle exit is not as appreciable as that of the circular nozzle.

4. Conclusion

In this study, experiments on jets were carried out under the steady discharge condition for various stagnation enthalpies with typical pressure 2.05 and 4.02 MPa, and many detailed data were obtained on the discharge flow rate, nozzle exit pressure, jet impingement force, and radial and axial pressure distributions of free and impingement jets. Principal results for each measured parameter are as follows.

(1) Discharged flow rate: The discharged flow rate data show that the prediction by Henry-Fauske's model can be in good agreement from the subcooled region to saturated steam, and an influence of nozzle entrance sharpness, namely the reduction of flow rate is little distinctive except for the highly subcooled region.

(2) Impingement force: Thrust coefficients based on the data for the round entrance circular nozzle are 1.1 $\sim$ 1.2 in the saturated region and approach about 1.95 with decreasing the stagnation enthalpy. For the sharp entrance nozzle, about 20% reduction is observed in comparison with the round entrance except near the saturated water.

(3) Recovery pressure distribution of jet: The data of axial and radial profiles show that characteristics of expansion and pressure decay highly depend on the stagnation enthalpy. For the subcooled region, expansion and pressure decay on the jet axis are delayed with decreasing the stagnation enthalpy, and the flashing core with high pressure is observed near the nozzle exit, and the marked expansion and steep decay of pressure result with disappearing of the core.

Furthermore, the core region becomes slightly longer when impinged on the plate. For the two-phase region, on the other hand, expansion and pressure decay initiate just downstream of the nozzle exit, and a dependence of pressure decay on the stagnation enthalpy is small. Comparing the data of elliptical nozzle with of circular nozzle, characteristics of central pressure decay near the nozzle exit are similar, however, flashing core lenth of the elliptical nozzle is slightly shorter. In addition, the approximate expressions of pressure decay on the jet axis were derived based on the data of circular nozzle.

5. Reference

[1] Kitade, K. et al., "Experimental study of pipe reaction force and jet impingement load at the break, "Paper F6/2 of 5th SMiRT, Berlin (August, 1979).

[2] Masuda, F. et al., "Experimental study and design evaluation of impengement steam jet, "Paper F6/10 of 6th SMiRT, Paris (August, 1981)

[3] Moody, F. J., "Maximus flow rate of a single component two-phase mixture, "J. Heat Transfer, ASME, Saries C. Vol. 87 (1965).

[4] Henry, R. E., Fauske, H. K., "The Two-Phase Critical Flow of One-component Mixture in Nozzles, Orifices, and Short Tubes," J. Heat Transfer, ASME, Series C, Vol. 93 (1971).

[5] Lienhard, J. H. Day, J. B., "The Breakup of Superheated Liquid Jets," J. Basic Engineering, ASME, Series D, Vol. 92 (1970).

[6] Forster, H. K., Zuber, N., "Growth of a Vapor Bubble in a Superheated Liquid," J. Applied Physics., Vol. 25 (1954).

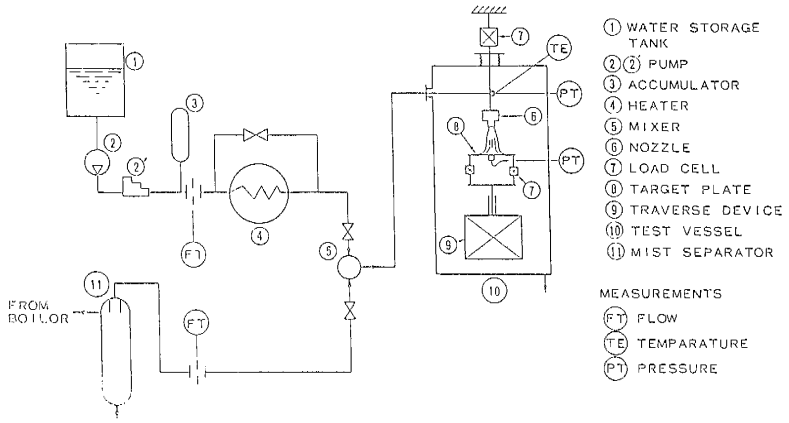

Fig. 1 Schematic diagram of experimental apparatus

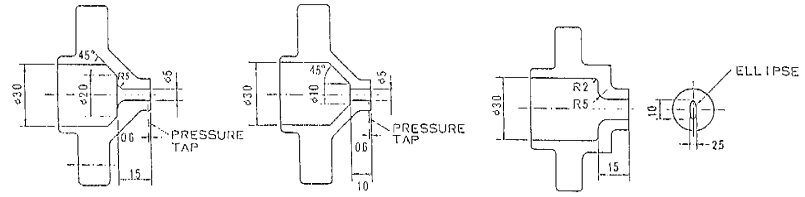

a) CIRCULAR NOZZLE (ROUND EDGE ENTRANCE)
(b) CIRCULAR NOZZLE (SHARP EDGE ENTRANCE)
(c) ELLIPTICAL NOZZLE

Fig. 2 Nozzle geometory

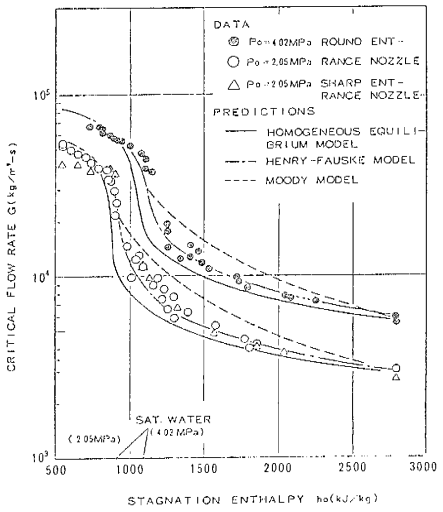

Fig. 3 Critica flow rate

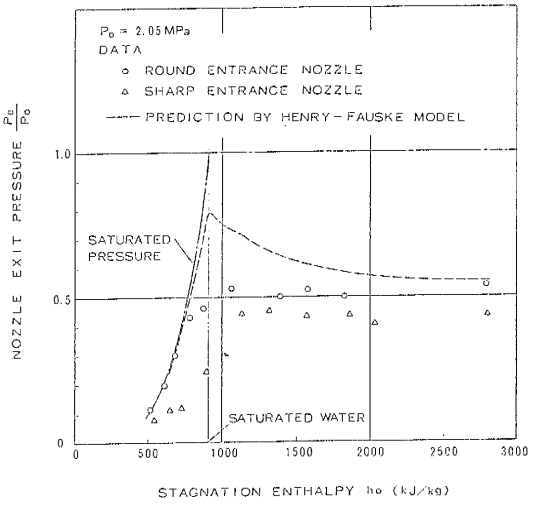

Fig. 4 Nozzle exit pressure

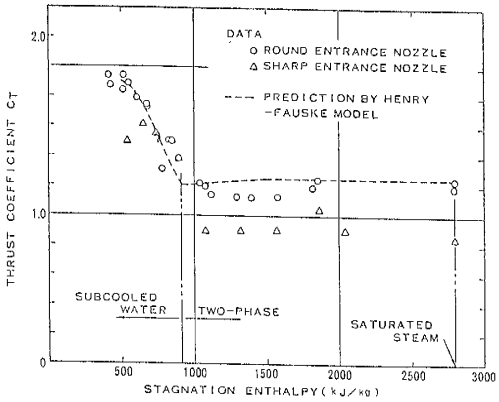

Fig. 5 Thrust coefficient for subcooled water and two-phase mixture

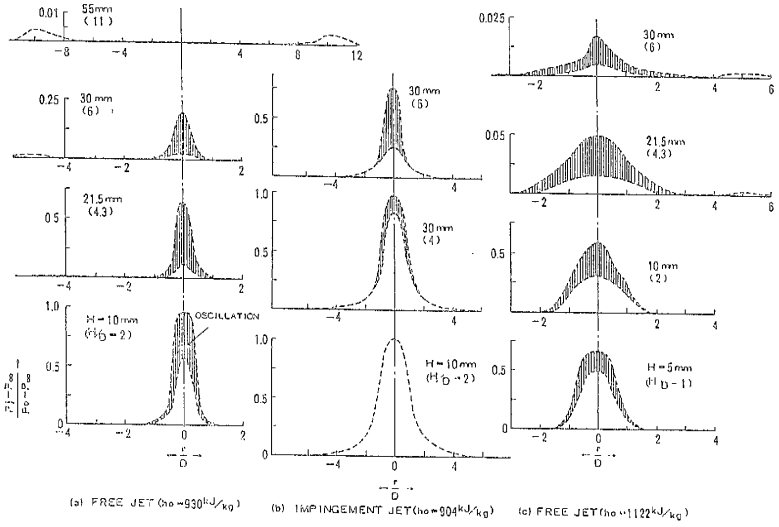

(a) FREE JET (h_o=930kJ/kg) (b) IMPINGEMENT JET(h_o=904kJ/kg) (c) FREE JET(h_o=1122kJ/kg)

Fig. 6 Radial pressure profiles (P_o=4.02MPa, CIRCULAR NOZZLE)

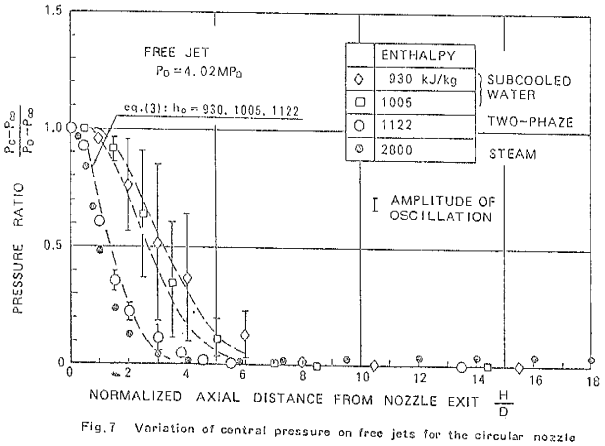

Fig. 7 Variation of central pressure on free jets for the circular nozzle

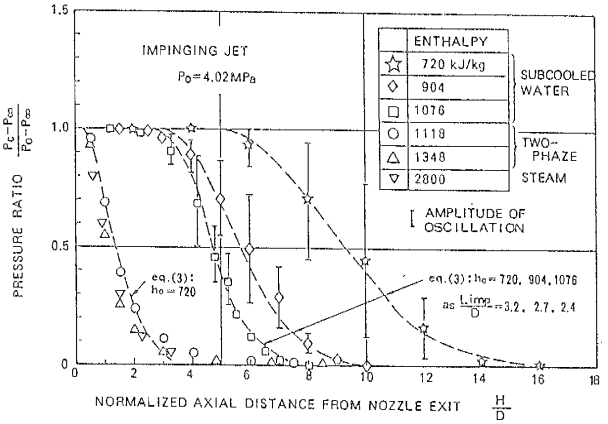

Fig. 8 Variation of central pressure on impingement jets for the circular nozzle

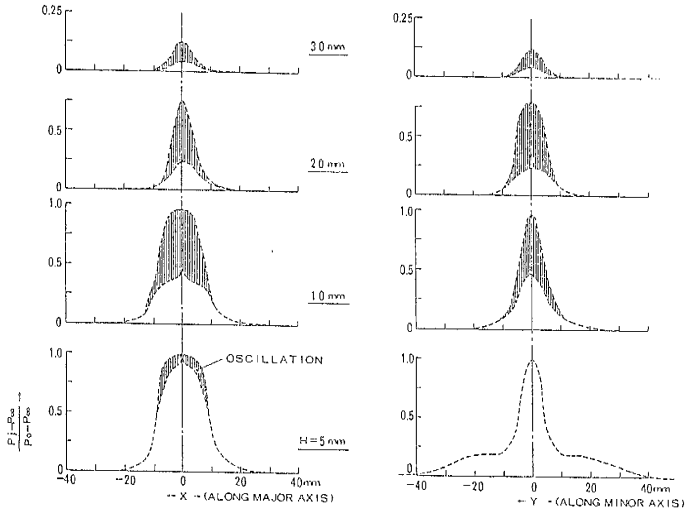

Fig. 9 Impingement Pressure Profiles for the elliptical nozzle(P_0=4.02MPa, h_0=925 kJ/kg)

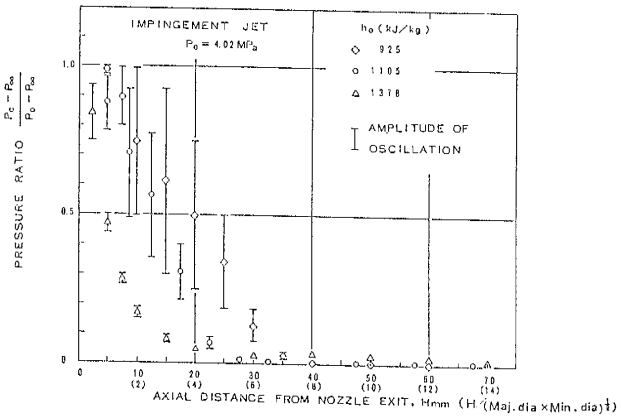

Fig. 10 Variation of central impingement pressure for the elliptical nozzle